

The Luminous Convolution Model for spiral galaxy rotation curves

S. Cisneros¹ ^{*}, J. G. O’Brien², N. S. Oblath¹, and J. A. Formaggio¹

¹ *Department of Physics, Massachusetts Institute of Technology, Cambridge, MA 02139, USA*

² *Department of Sciences, Wentworth Institute of Technology, Boston, MA 02130, USA*

16 November 2021

ABSTRACT

The Luminous Convolution Model (LCM) is an empirical formula, based on a heuristic convolution of Relativistic transformations, which makes it possible to predict the observed rotation curves of a broad class of spiral galaxies from luminous matter alone. Since the LCM is independent of distance estimates or dark matter halo densities, it is the first model of its kind which constrains luminous matter modeling directly from the observed spectral shifts of characteristic photon emission/absorption lines. In this paper we present the LCM solution to a diverse sample of twenty-five (25) galaxies of varying morphologies and sizes. For the chosen sample, it is shown that the LCM is more accurate than either Modified Newtonian Dynamics or dark matter models and returns physically reasonable mass to light ratios and exponential scale lengths. Unlike either Modified Newtonian Dynamics or dark matter models, the LCM predicts something which is directly falsifiable through improvements in our observational capacity, the luminous mass profile. The question, while interesting, of if the LCM constrains the relation of the baryonic to dark matter is beyond the scope of the current work.

The focus of this paper is to show that it is possible to describe a broad and diverse spectrum of galaxies efficiently with the LCM formula. Moreover, since the LCM free parameter predicts the ratio of the Milky Way galaxy baryonic mass density to that of the galaxy emitting the photon, if the Milky Way mass models can be trusted at face values, we then show that the LCM becomes a zero parameter model. This paper substantially expands the results in arXiv:1309.7370 and arXiv:1407.7583.

1 INTRODUCTION

Flat rotation-curve observations of spiral galaxies have long been considered the smoking gun for the existence of dark matter to account for the missing mass problem (Rubin et al. 1978; Bosma 1978). In recent years novel new techniques have been employed in the search for dark matter. However at the present moment, without the parameter space being reduced, the lack of pure evidence has paved the way for researchers to explore alternative gravitational models. Many of these theories such as Modified Newtonian Dynamics (MOND) (Milgrom 1983) and Conformal Gravity (Mannheim & O’Brien 2012) have shown success and shortcomings. Here, we present a new prescription, the Luminous Convolution Model (LCM), for calculating galaxy rotation curves using a modified velocity addition formula with only luminous matter. The LCM is consistent with Special and General Relativity (SR+GR), though uses new applications of these familiar concepts.

Traditionally, the relative curvature effects, i.e. gravitational redshifts of a photon from the spiral galaxy where it is emitted with respect to where it is received, are neglected as too small to impact the total rotation curve magnitudes. However, such relative curvatures effects are evaluated by taking the algebraic difference of the gravitational redshifts

of the two galaxies in question. We posit that this classical subtraction of gravitational redshifts is a Galilean concept, and therefore not applicable to light. Since light remains invariant under Lorentz transformations, not Galilean, we re-calculate the relative curvature effects from luminous matter using Lorentz-type transformations in order to relate the relative galaxy frames. The equivalent doppler shifts for the emitter galaxy relative to the receiver galaxy (the Milky Way) are then re-phrased kinematically, and we show how this new effect can account for the missing rotational velocity in an arbitrary spiral galaxy.

In a sample of twenty-five (25) well studied galaxies the Luminous Convolution Model (LCM) fits rotation curves more accurately than either Modified Newtonian Dynamics (MOND) or dark matter halo (DM) fits. The LCM is an empirical formula which predicts the observations of spiral galaxy rotation curves with reasonable estimates of the luminous mass, across the samples broad range of sizes and morphologies without modifying classical laws of gravity. Additionally, the LCM is a potentially falsifiable model, through comparisons between observations and the density predictions of the luminous mass made from the LCM free parameter. In this paper, our analysis is focused on the highly symmetric case of spiral galaxies (in the plane of the galac-

tic disk), but it should be noted that the theoretical LCM mapping basis can in theory be analytically extended to arbitrary geometries (Cisneros et al. 2013). Examples of physical systems where LCM constructions will be considered in future work, which are beyond the scope of the current paper, include galaxy mergers, clusters of galaxies, lensing, and elliptical galaxies.

This paper is organized as follows: Sec. 2 is the summary description of the LCM mapping formalism, Sec. 3 presents the sample and results, Sec. 4 presents conclusions and possible future directions and Sec. 5 gives acknowledgements and an appendix with a detailed LCM heuristic derivation.

2 LORENTZ KINEMATICS AND THE LCM ROTATION CURVE FORMULA

To account for the missing mass in spiral galaxies, DM theories contain a contribution of rotational velocity from the dark masses, resulting in the rotation curve formula,

$$v_{rot}^2 = v_{lum}^2 + v_{dark}^2, \quad (1)$$

where v_{lum} is the contribution expected from photometric observations of the luminous matter (disk, bulge and gas). The typical functional form of the expected value of v_{lum} is the Freeman formula,

$$v_{lum}^2 = \frac{N^* \beta^* c^2 R^2}{2R_0^3} F(R) \quad (2)$$

where R_0 is the galactic scale length and N^* is the number of stars in the galaxy. The function F is given by

$$F(R) = \left[I_0 \left(\frac{R}{2R_0} \right) K_0 \left(\frac{R}{2R_0} \right) - I_1 \left(\frac{R}{2R_0} \right) K_1 \left(\frac{R}{2R_0} \right) \right], \quad (3)$$

where I_0 , I_1 , K_0 , and K_1 are the standard modified Bessel functions. Although the dark matter contributions are not detectable by any current means, the relative amounts in each galaxy are inferred by the difference between the expected luminous mass contribution and the total rotation observations, v_{obs} , which comes from measurements of Doppler shifted spectra. Hence the sum v_{rot} is the DM prediction which is fit against the actual measured velocity v_{obs} .

The functional forms of the two terms in Eq. (1) have been well established (see for example (Mannheim 2006)) and usually provide an accurate statistical fit to the data. However, since the luminous contribution can only typically account for the inner region of spiral galaxies, the dark component dominates the outer regions, and fits the data with two free parameters per galaxy.

In our prescription, the Lorentz Doppler shift formula (LD)

$$\frac{v_{obs}(r)}{c} = \frac{\frac{\omega'(r)}{\omega_o} - \frac{\omega_o}{\omega'(r)}}{\frac{\omega'(r)}{\omega_o} + \frac{\omega_o}{\omega'(r)}}, \quad (4)$$

which acts to convolve the frequency ω' (received from a moving frame) with the characteristic rest frame frequency ω_o . Then ω_o is generalized so that the resulting velocity parameter v_{obs} in Eq. (4) is interpreted as the underlying Lorentz transformation which rotates a photon's four-vector between the two frames. It is from this formula which we will derive a luminous photometric profile that will match v_{obs} ,

by rotating between the two slightly curved galactic frames of spiral galaxies, based on decomposing the total observed Doppler-shifted frequencies ω' into two contributions: the relative velocity and the relative curvature.

Hence, the LCM modifies the velocity addition formula in Eq. (1) by replacing the DM halo velocity contributions, v_{dark}^2 , with the relative curvature convolution \tilde{v}_{lcm}^2 . It has been shown in previous work (Cisneros et al. 2015; Radosz et al. 2013) that curvature effects can be phrased kinematically. The LCM prediction of the total observed shifted frequencies, ω' interpreted via the LD, is then :

$$v_{rot}^2 = v_{lum}^2 + \alpha \tilde{v}_{lcm}^2, \quad (5)$$

where v_{lum}^2 remains the expected relative velocity (Freeman) contribution, v_{rot} is the LCM prediction which is fitted to the total reported v_{obs} , and α is the LCM free fitting parameter. Although in the original work on the LCM (Cisneros et al. 2013), α was a purely free parameter, in this work we will show that instead it is highly correlated to the dimensionless ratio

$$\alpha = \left(\frac{\rho_{mw}}{\rho_{gal}} \right)^{1.64} \quad (6)$$

of the radial densities of the photon receiving galaxy (Milky Way) ρ_{mw} to the photon emitting galaxy ρ_{gal} . Here, the radial density is defined by:

$$\rho = \frac{M_{total}}{r_e}, \quad (7)$$

for M_{total} the integrated total luminous mass at the limit of the reported data, and r_e the exponential scale-length (described in Sec. 2.2) for that baryonic mass distribution.

2.1 LCM relative curvature convolution

Relative curvatures for the spiral galaxies presented in this work are defined as a function of radius r from the center of the galaxy, with the Schwarzschild metric gravitational redshifts via:

$$\frac{\omega_o}{\omega(r)} = \left(\frac{1}{\sqrt{-g_{tt}}} \right)_r. \quad (8)$$

Here, ω_o is the characteristic photon frequency (defined in Eq. 4), and $\omega(r)$ is the shifted frequency due to the gravitational curvature¹. The temporal Schwarzschild metric coefficient g_{tt} is defined as the usual:

$$g_{tt}(r) = - \left(1 - 2 \frac{GM}{c^2 r} \right), \quad (9)$$

where G is Newton's constant of gravity, M is the Gaussian enclosed mass at some radial distance r from the center of the mass distribution, and c is the vacuum light speed. In the weak field limit (Hartle 2003), the temporal metric Eq (9) takes the form of

$$g_{tt}(r) \approx -1 + 2 \frac{\Phi(r)}{c^2}. \quad (10)$$

Here, Φ is the usual Newtonian scalar gravitational potential. Spiral galaxies as a whole can be treated gravitationally as weak fields due to the diffuse nature of the luminous mass

¹ as received by a stationary observer at asymptotic infinity

distributions. This has served to motivate the common use of the classical Poisson equation in DM theories. For the LCM, this serves to justify the use of the Lorentz transformation architecture to map the slightly curved frames of spiral galaxies.

While the relative curvature estimates we use are precisely those which have previously been obviated as too small to impact rotation curve velocities, we should note the difference between the LCM and previous treatments which have ruled out curvature contributions from luminous matter. Namely, previous treatments considered relative curvature effects by simply taking the difference of the magnitudes of the two gravitational redshifts between the photon source (the emitting galaxies) and the Milky Way (receiving galaxy). This over-simplified explanation is one that is Galilean in nature and will in turn be inadequate. This can be easily rectified since light is a Lorentz invariant and so requires a relativistic transformation to relate any relative effects that could arise from curvature, even if they are weak.

The entire LCM heuristic mapping derivation is described in Appendix A, but here for continuity we present the resulting \tilde{v}_{lcm}^2 :

$$\tilde{v}_{lcm}^2 = \kappa^2 v_1 v_2, \quad (11)$$

where κ is the curvature ratio which scales the coordinate time of the emitter galaxy relative to that of the Milky Way:

$$\kappa(r) = \frac{c - \tilde{c}_{gal}(r)}{c - \tilde{c}_{mw}(r)}, \quad (12)$$

by multiplying each factor of c which results from the successive v_1/c and v_2/c Lorentz-type transformations. The terms $\tilde{c}_{gal}(r)$ and $\tilde{c}_{mw}(r)$ are the respective coordinate light speeds of the emitter and receiver galaxies. These coordinate light speeds are a physical indicator of curvature, specifically the degree to which path lengths are increased due to curvature. We then define \tilde{c} in terms of the Schwarzschild metric relation:

$$n(r)\tilde{c} = \left(\frac{1}{\sqrt{-g_{tt}}} \right)_r \tilde{c} = c. \quad (13)$$

The Lorentz-type transformation v_1 acts to map the two galactic frames as a function of radius:

$$\frac{v_1}{c} = \left(\frac{1}{\cosh \xi_c} - 1 \right) = \left(\frac{2}{e^{\xi_c} + e^{-\xi_c}} - 1 \right), \quad (14)$$

for the fundamental mapping kernel:

$$e^{\xi_c}(r) = \frac{\omega_{mw}(r)}{\omega_{gal}(r)}. \quad (15)$$

The respective frequencies ω_{mw} and ω_{gal} are the gravitational redshift frequencies defined by $\omega(r)$ in Eq. 8 as a function of r .

The second Lorentz-type transformation v_2 maps from the curved two frame of Eq. 15 to the the associated flat frames where photons are emitted and received:

$$\frac{v_2}{c} = 1 / \tanh \xi_2 = \frac{(e^{\xi_2})^2 + 1}{(e^{\xi_2})^2 - 1}, \quad (16)$$

for the fundamental mapping kernel:

$$(e^{\xi_2})^2 = \frac{e^{\xi_f}}{e^{\xi_c}}. \quad (17)$$

Lastly, the flat 2-frame mapping is defined by

$$e^{\xi_f}(r) = \frac{\omega_l(r)}{\omega_o}, \quad (18)$$

which allows for our contribution \tilde{v}_{lcm}^2 to be calculated and then used in Eq. 5 to give the entire LCM prediction for the rotational velocity of the galaxy in question.

2.1.1 Note on integration constants and physicality:

The gravitational potential, $\Phi(r)$, which parametrizes the curvatures of interest in Eq. 10, is defined as an integral over the Newtonian force $F(r)$:

$$\Phi(r) - \Phi_o = - \int \frac{F(r)}{m} dr, \quad (19)$$

where $F(r)/m$ is the force per unit mass for each individual luminous mass component, and Φ_o is the integration constant of interest.

This integration constant is generally set such that the potential $\Phi(r) \rightarrow 0$ as $r \rightarrow \infty$. However, when considering two arbitrary galaxies², connected by a single photon, it is a violation of energy conservation to set the respective integration constants to different values. We select a single universal value for the integration constant, taken to be zero. It is beyond the scope of this paper to find a more accurate choice, but it should be considered that a more physical choice may be found in future dark energy research. Physically, our assumption means that at large r the gravitational potentials return the familiar small but non-zero values.

2.2 LCM rotation curve fitting protocol

With the basis for the LCM contributions established, we can then fit the predicted LCM rotation curve velocity v_{rot} (Eq.5) to the reported rotation curve data v_{obs} (Eq. 4). The LCM prediction and fit are calculated using the MINUIT minimization software as implemented in the ROOT data-analysis package (Brun & Rademakers 1997). The fitting procedure can be summarized as follows:

(i) The luminous mass components reported in each reference (gas, disk, bulge) are digitized using the software package Graph Click (GraphClick 2013);

(ii) The associated Newtonian gravitational potential Φ is calculated for each component and the components are summed (Eq 19);

(iii) The Schwarzschild metric is then parametrized by the luminous mass distribution as a function of radius, and the convolution function, v_{lcm} , is calculated in comparison to the Milky Way luminous mass profile;

(iv) The minimization procedure explores the parameter space to find an optimal luminous profile (v_{obs}) from the data (v_{rot}). This process can be iterated within the bounds of reported mass-to-light ratios, distances and scale lengths.

(v) The resulting best-fit values for luminous mass profile (indicated by the rotation curve data) is then fit to return an exponential scale length r_e for a smoothed profile including

² the emitter galaxy and the receiver galaxy (Milky Way)

gas, disk and bulge, and the total mass of the emitter galaxy. A sample of the output is shown in Fig. 1 ;

(vi) The correlation over the entire sample of the α parameter to the density ratio in Eq. 7 is then used to ascertain the global value of the receiving (Milky Way) galaxy's scale length r_e as reported in Table 3 for five different Milky Way luminous mass models.

It is important to note that a unique feature of the LCM is contained in steps (iv) and (v) above. Unlike most alternative dark matter models, we use the LCM formalism to predict a luminous profile for the given galaxy. Hence, when the LCM returns the convolution function, it is fit to the observed data and then we extract a scale length and a luminous mass in step (v). These values are reported in Table 2. These values act as a prediction for the galaxy in question and then can be compared with established results from photometry and population synthesis modeling. This feature sets the LCM apart, since we do not use the scale length or mass as input for the galaxy, and thus have a testable result for each galaxy fit by the LCM. As mentioned above in step (iv), in this current work we fit the entire returned luminous profile of the galaxy with a thin luminous disk to return estimates of the total luminous mass and exponential scalelength r_e . Although some of the galaxies may contain a documented bulge, as noted in Table 2 by an asterisk (*), the main differentiating feature between observation and Keplerian prediction occurs in regions outside the bulge (usually after the peak velocity which typically occurs at $r = 2.2r_e$). Since most bulge contributions fall off quickly, in general $r_b < r_e$, then for this work as a test of concept, we kept the fits described in step (iv) (to the Luminous mass profile resulting from step (iii)) simple while still obtaining physically acceptable results. Future testing will require more rigor of implementing the resulting profiles and testing the full bulge and HI data of each of the galaxies. Since the LCM requires information about the emitter galaxy as well as the receiver, then it should be noted that the LCM is not only sensitive to the data used of the emitter galaxy, but also the data used for our own milky way. To avoid bias as well as make the LCM more robust, we have run the sample of emitter galaxies against five different, well studied, Milky Way luminous mass profiles.

As expected, the luminous mass profiles resulting from step (iv) above shows variation pending the choice of the Milky Way luminous profile used in the mappings. However, it should be noted that this is not a pure fitting alone. The fits returned come with physical quantities such as the luminous mass and the galactic scale length which can be compared with astronomical data. The fit to NGC 3198 shown in Fig. 1 is quite a remarkable fit due to the fitting procedure, but more importantly is physically acceptable. The fit shown returns both a luminous mass and a scale length which is consistent with documented sources (de Blok et al. 2008), and is recovered from Eq. 5 without the need for any dark matter. Moreover, since estimates of the Milky Way's baryonic content are notoriously difficult to determine, this demonstrates that the LCM can be used to distinguish between different estimates of the Milky Way's luminous mass for a given sample while all other factors are held constant (ie. extent of reported coverage, etc), see Sec. 3.4. Moreover, this feature can be leveraged if the data from the emitter

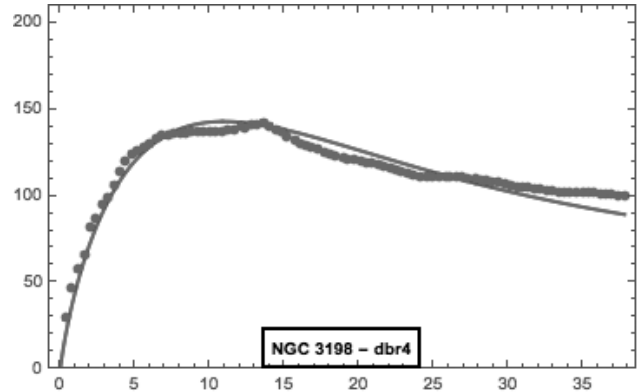


Figure 1. The fit returned in steps (iii) through (v) of the LCM fitting procedure for NGC 3198. Galaxy name appended with dbr4 indicates original luminous mass model from de Blok et al. (2008) and the fourth run against the data, where each run iterates the luminous mass profile to reflect the observed spectral line shifts in the reported data.

galaxies is accurate and the LCM is empowered, then results over a reliable sample of galaxies can be used to infer validity of Milky Way data. Since the LCM requires information about the emitter and receiver galaxy, the returned luminous profile in steps (v) and (vi) above are specific to the reported data, at the assumed distance. If either variable is changed, the luminous mass must therefore compensate accordingly.

3 RESULTS

3.1 The sample

The LCM sample reported in this paper represents twenty-five (25) galaxies selected to represent a broad spectrum of morphologies and luminous mass density profiles. It can be seen in Table 2 that the sample also encompasses a large variation in estimated distances as well as overall size of the galaxies. Having such a diverse sample allows the LCM to illustrate its modeling power. Typically in DM theories the morphology of the galaxy (such as dwarf or large spiral) dictates the relative location of the DM and thus changes the corresponding function which fits the data. This occurs also in competing alternative theories such as MOND, where the choice of the interpolation function can be dictated by properties such as the morphology or the distance. Here we show that the LCM can account for the missing mass discrepancy in each of the galaxies in a more universal manner. It should also be noted that the chosen sample is comprised of some of the most well studied galaxies in rotation curve physics, making the sample as unbiased and reliable as possible (Persic et al. 1996). We also report in Table 2 the original sources of the rotation curve data for more specific information on a particular galaxy.

Results for each emitter galaxy are given in Table 2, including: α , M/L, r_e , the LCM reduced χ^2 , the reduced χ^2 values for the DM or alternative gravity model which was originally fit to the same data. The M/L reported here reflect the smoothed profile including the gas, bulge and disk together, as noted in Sec. 2.2. All result values and

rotation curve figures (Fig. 4 - 6) reported here reflect the mapping to a Milky Way luminous mass model synthesized from the Xue et al. (2008) disk and Sofue (2013) bulge. More information on the Milky Way data sets are described in Sec. 3.4. As can be seen in Fig. 4 - 6, the relative curvature contribution serves to correct the rotation curve and provide outstanding fits. Furthermore since the relative curvature contribution is unique to the Milky Way, and is not described by any free parameters, it makes the fits shown in Fig. 3-5 very accurate and falsifiable because unlike MOND and dark matter models, the LCM predicts something which we can measure, the baryonic mass.

3.2 Adopted Distances

It is important when fitting rotation curves to any theory that a solid understanding of the estimated distances to the galaxy is provided. As mentioned in the previous section, many alternative theories are quite sensitive to distance modifications to the galactic data since photometric properties such as scale length and luminosity are completely dependent on the assumed distance when the data is taken by an astronomer. In order to keep the systematics of this work standardized, we will adopt the most common value for the distances to each galaxy captured in the literature. For most of the sample, this means that we are keeping the original distances quoted by the astronomers, with the exception of some of the Ursa Major Galaxies whose distances have been significantly modified in recent work (Sanders & McGaugh 2002). We note that the LCM, like most other theories is sensitive to the distance used. However, in this work we have shown in Table 2 that using the quoted distances the LCM is able to return physically reliable scalelengths and mass to light ratios. Mannheim & O'Brien (2012) provides an extensive discussion on how to adjust rotation curve data via updated observable parameters such as distances and inclinations, where they use a standard of adopting only distances based on either cepheid data or an averaging over the NASA Extragalactic Database (NED). In this work we kept true to the quoted distances to show that physical solutions are possible in the LCM, but it should be noted that updated distances are obtained, all the quoted parameters in Table 2 will scale accordingly.

3.3 Error estimates and reduced χ_r^2 values

All figures reported here indicate the uncertainties reported in the literature. There is currently no standard practice as to how to quantify the uncertainties associated with rotation curve data (Gentile et al. 2011; de Blok et al. 2008; Navarro 1998; Sanders 1996), such that χ_r^2 values do not indicate global goodness of fit between data sets, but can be used to distinguish models applied to the same data set. Generally the uncertainties in this paper come from either statistical errors from tilted ring model fits to the H I velocity fields or differences between the approaching- and receding-side velocity fields (de Blok et al. 2008; Gentile et al. 2011; Randriamampandry & Carignan 2014). In Table 2 we show that χ_r^2 values are consistently lower for LCM fits than for

those of the reporting models. We use the same comparison of χ_r^2 , though averaged across the entire sample to compare different Milky Way luminous mass models, as indicated in Sec. 3.4.

3.4 Milky Way luminous mass models and identification of the α parameter

In the LCM we map each emitter galaxy onto the receiver galaxy (i.e. the Milky Way) to derive the relative curvature contribution, v_{lcm} , to the total measured rotation curve. Since we are making observations of photons from the inside of the system, the luminous matter profile of the Milky Way is difficult to determine and constrain (e.g. interpreting H I Carignan & Chemin (2006)). We have compared each emitter galaxy in our sample of twenty-five (25) galaxies to four (4) different Milky Way luminous mass models, to accommodate these differences in Milky Way (MW) luminous mass estimates; Sofue (2013), Xue et al. (2008) and two models from Klypin et al. (2002). Table 1 and Fig. 3 show the differences between the various MW models graphically and numerically.

As can be seen in Table 1, these MW models differ primarily in the inner mass contributions and generally asymptote to similar values at large radii. We have found that in the cases of the Klypin and Xue MW models, the lower inner velocity profile preclude fitting very dense central mass distributions in galaxies such as NGC 2841, NGC 7814, NGC 7331 and NGC 5055. For the Xue model, the α parameter can be constrained to return reasonable fits to all of these galaxies. However, it is the Sofue MW which fits all galaxies in our sample with no artificial bounding on the free parameter. Since one advantage of the Xue MW is the extent of the radial coverage, we have synthesized a MW from the Sofue bulge and the Xue disk, which allows us to fit all galaxies in our sample to their furthest extent, while still taking advantage of the central mass concentration reported in the Sofue MW. Since one of the goals of the current paper is to identify the physical interpretation of the LCM free parameter α , then fitting the galaxies to various MW models helps us to constrain and eventually fix α .

The identification of the LCM free parameter α as highly correlated with the function Eq. 6 can now be explored. We fit the distribution of the LCM α results against the emitter galaxy radial densities (defined in Eq. 7) with a power law. The power law fits result in an average value for the exponent of 1.64 (see Figure 2). While it is notably coincidental that this exponent is similar to those often reported for the dark halo density parameters in NFW models (Navarro et al. 1997), we do not in this paper make any comments or claims to any relationship with the NFW. However, since all DM or alternative gravitational theories are seeking to explain the same physics, via differently described phenomena, coincidences as such are both unavoidable and beneficial to the entire community to spark dialogue of overlap and plausibility. The result of the fits to the α distribution for the entire sample has given the LCM a way to predict the scale length of the given MW model, given that we use the masses reported for each model. The LCM prediction for the MW scalelengths are reported in Table 3, along with the corresponding χ_R^2 value for each MW power law fit. We note that while the Xue/Sofue MW is not the best χ_R^2

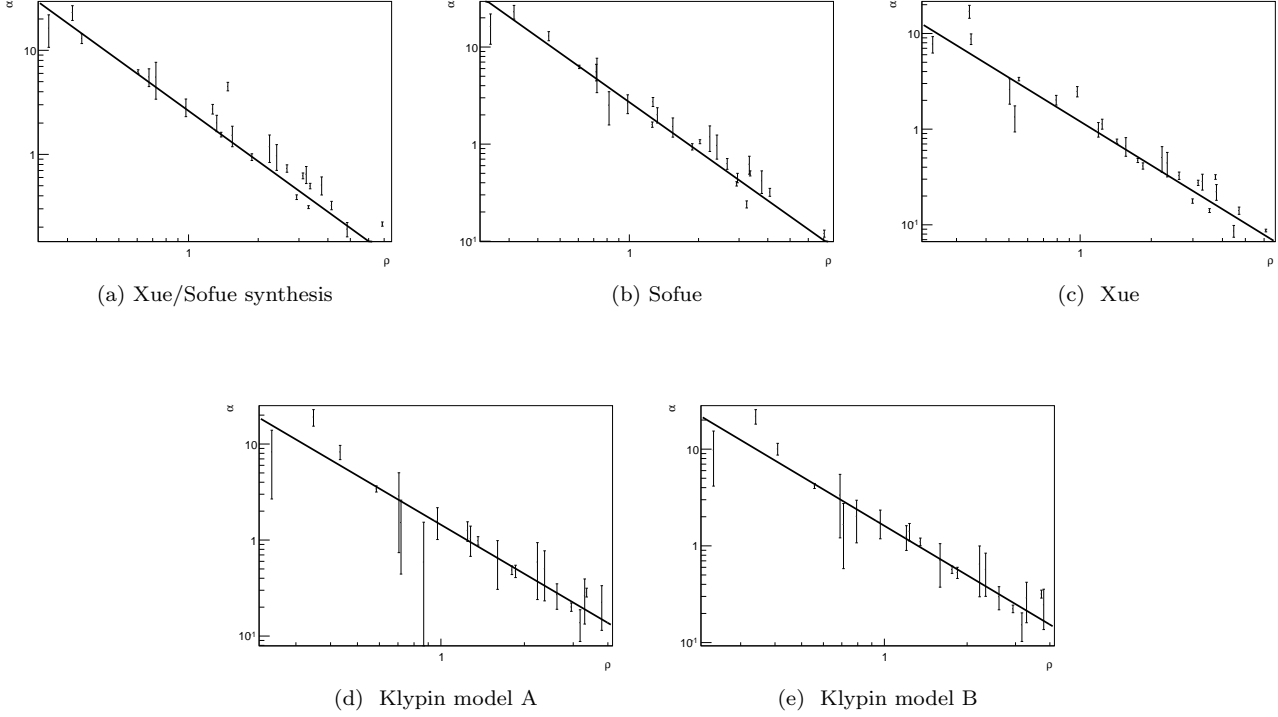


Figure 2. Log-log plot of the LCM distribution of α versus radial density ρ_r (Eq. 7) for one Milky Way to the sample of photon emitter galaxies, each dot represents one such galaxy mapped to the Xue/Sofue synthesized Milky Way. Errors are statistical only.

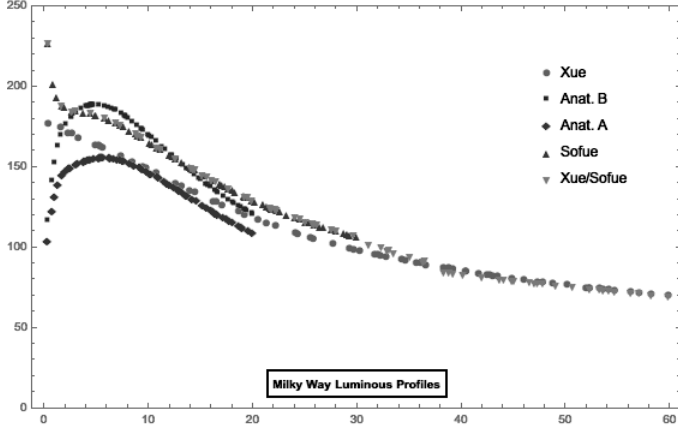


Figure 3. The Milky Way orbital velocities due to the luminous mass profiles reported in each of the four references used in this work, as well as the Milky Way synthesized from Xue/Sofue.

value, it does fit all emitter galaxies in the sample without artificial constraints on the bounds for the α parameter.

4 CONCLUSIONS

We posit that what is presented in this paper will help to constrain the Milky Way mass models. The only free parameter α in Eq. 6, has been shown to high confidence to be the ratio of the radial densities of the Milky Way to emitter galaxy (that galaxy from we are measuring the photons). This conclusion makes the current version of the LCM quite

Table 1. Milky Way Luminous Mass Models & α analysis

Galaxy	R_{last}	M_{bulge}	M_{disk}	b	r_e	χ_R^2	dof
Xue/Sofue	60kpc	1.8	5.30	1.611	3.74	13.19	24
Sofue	30 kpc	1.8	6.80	1.683	4.76	6.52	23
Xue	60 kpc	1.5	5.00	1.523	5.76	11.45	24
Klypin, A	15 kpc	0.8	4.00	1.699	3.87	1.76	20
Klypin, B	15 kpc	1.0	5.00	1.696	4.53	2.65	20

Masses in units of $10^{10} M_\odot$, exponential scalelengths r_e in (kpc), predicted from fit values of b , for power law fits of the form $\alpha = (\rho_{mw}/\rho_{gal})^b$. Goodness of fit indicated by reduced χ_R^2 values per degrees of freedom (dof).

powerful in relation to both DM theories and other alternative gravitational models. Furthermore, as can be seen in Fig. 4-6, the rotation curves are predicted at the documented values reported in Table 2, without the need for invoking any dark matter. This is because, the relative curvature contributions allow that the luminous mass profile can be extracted from the observed spectra shifts of light. It has been noted by Bottema et al. (2002) that a credible, empirical alternative to DM must:

- successfully predict rotation curves with reasonable estimates of the stellar mass-to-light ratios and gas fractions
- make sense within our physics framework
- have fewer free parameters or have one universal parameter
- predict various other astrophysical observations.

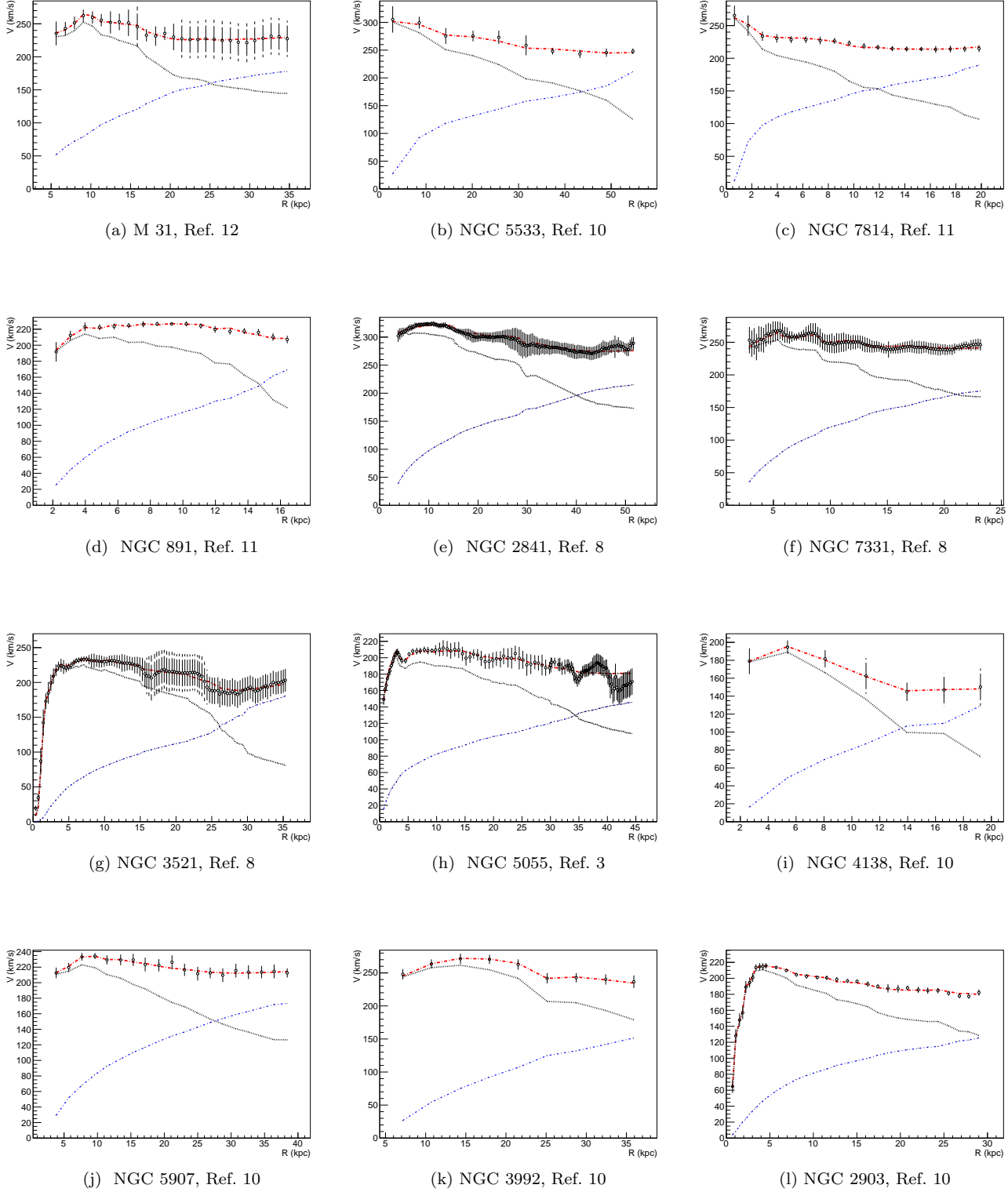


Figure 4. LCM rotation curve fits. In all panels lines are; circles with associated error bars is reported data, red dotted-dashed is LCM fit to the reported data, blue dotted-dashed is relative curvature contribution and the black dotted line is the Keplerian prediction from the luminous mass. References are as in Table 2.

Table 2. Results for originating model and LCM

Galaxy	Ref.	Distance	Luminosity	Other fit results		LCM fit results			
		(Mpc)	$10^{10} L_{\odot}$	Model	χ_r^2	α	M/L	r_e	χ_r^2
F 563-1	2	45	0.15	NFW	0.05	5.53	12.53	2.60	0.02
M 31*	12	0.78	2.60	ISO	0.36	0.65	5.96	4.80	0.04
M 33	5	0.84	0.57	NFW	2.46	13.01	0.88	1.46	0.14
NGC 891*	11	9.5	2.50	MaxLight	1.10	0.94	3.11	4.14	0.25
NGC 925	3	9.25	1.61	ISO	2.40	23.10	0.85	4.35	0.07
NGC 2403	3	3.22	0.93	NFW	4.56	6.25	1.42	2.18	0.56
NGC 2841*	6	14.1	4.74	CG	2.27	0.21	5.46	3.77	0.11
NGC 2903	10	6.4	3.66	MOND	10.71	0.39	2.03	2.53	0.31
NGC 3198	3	13.8	3.24	NFW	5.40	1.55	1.88	4.41	0.26
NGC 3521	6	10.7	4.77	CG	1.37	0.62	2.15	3.29	0.22
NGC 3726	10	18.6	3.77	MOND	3.57	2.86	1.04	4.02	0.27
NGC 3953	10	18.6	4.19	MOND	1.35	0.97	1.93	3.36	0.32
NGC 3992	10	18.6	7.50	MOND	0.50	0.51	2.34	4.66	0.03
NGC 4088	10	18.6	0.88	MOND	1.70	1.52	6.41	3.65	0.27
NGC 4138	10	18.6	1.18	MOND	2.12	1.19	2.93	1.55	0.01
NGC 5055*	3	10.1	3.62	NFW	17.23	0.31	3.01	3.30	0.53
NGC 5533*	10	54	4.5	MOND	1.57	0.19	7.58	7.04	0.22
NGC 5907*	10	18.6	7.20	MOND	0.44	0.73	1.87	5.05	0.10
NGC 6946*	10	6.9	2.73	MOND	3.03	2.73	1.42	3.04	0.14
NGC 7331	6	14	6.77	CG	1.24	0.50	1.48	2.98	0.10
NGC 7793	14	3.38	0.31	ISO	1.08	5.56	2.51	1.15	0.06
NGC 7814*	11	14.6	1.30	ISO	0.25	0.32	4.38	1.37	0.15
UGC 128	6	64.4	4.60	CG	1.08	4.50	2.62	8.14	0.19
UGC 6973	10	18.6	0.89	MOND	23.5	2.01	1.27	0.86	0.02
UGC 7524	6	4.12	0.37	CG	0.39	16.30	2.23	3.32	0.06

Values in this table are reported for the galaxy pairings to the Milky Way synthesized from Xue et al. (2008) and Sofue (2013). Mass-to-light ratios in units of M_{\odot}/L_{\odot} . Reduced χ^2 per degree of freedom indicated by χ_r^2 . Galaxies for which the original literature reported a bulge component are indicated by (*). Other models include the dark matter halo models (NFW and ISO), Conformal Gravity (CG), MOND modified Newtonian Dynamics (MOND) and maximum disk (baryonic) mass model (MaxLight).

References: 1. Begeman (1989), 2. Navarro (1998), 3. de Blok et al. (2008), 4. Gentile et al. (2013), 5. Corbelli (2003), 6. Mannheim & O’Brien (2013), 7. Battaglia et al. (2006), 8. Gentile et al. (2011), 9. Bottema et al. (2002), 10. Sanders & McGaugh (2002), 11. Fraternali et al. (2011), 12. Carignan & Chemin (2006), 13. Giraud (2000), 14. Dicaire et al. (2008).

While the LCM has not yet been extended to other astrophysical observations, at this early stage of development in proof of concept, the LCM does the first three very well.

To predict other astrophysical phenomena, the geometrical construction here in the context of high symmetry must be extended to other more complex situations. In future work the first places the LCM can be applied is to a statistical constraint to the Milky Way luminous mass models and to weak lensing. The LCM is already constructed for testing the first case and in the second, (Narayan et al. 1997) have already phrased the weak lensing problem in similar curvature terms. Two very interesting next directions include investigations of the coincidence between the dark matter halo density exponent and that of the interpretation of the LCM free parameter α given in Eq. 6, and fitting the rotation curve of the Milky Way itself. Since the LCM formalism is based upon the conjecture that the frame-dependent effects of the Milky Way’s luminous mass profile are convolved into our observations of spectral shifts, analysis of the Milky Way rotation curve itself will rely upon rephrasing the LCM construction in the case where the observer’s frame is imbedded in the emitter’s global frame. The LCM is potentially falsifiable in any of these cases, and eventually

once it has been tested in a larger sample of galaxies, could be in principle extended numerically to an arbitrary metric case of dynamics to include galaxy mergers and galaxy clusters. In the immediate context, the LCM is a robust model which constrains the luminous matter modeling of galaxies directly from spectra, under the assumption of a Milky Way luminous mass profile in a manner that is void of free parameters.

5 ACKNOWLEDGMENTS

The authors would like to thank R. A. M. Walterbos, V. P. Nair, M. Inzunza II, J. Conrad, V. Papavassiliou, T. Boyer, P. Fisher, E. Bertschinger, I. Cisneros, S. Nabahe, D. Wilmot, T. Robertson and R. J. Moss.

S. Cisneros has received support from the MIT Martin Luther King Jr. Fellowship throughout this work, while J. A. Formaggio and N. A. Oblath are supported by the United States Department of Energy under Grant No. DE-FG02-06ER-41420.

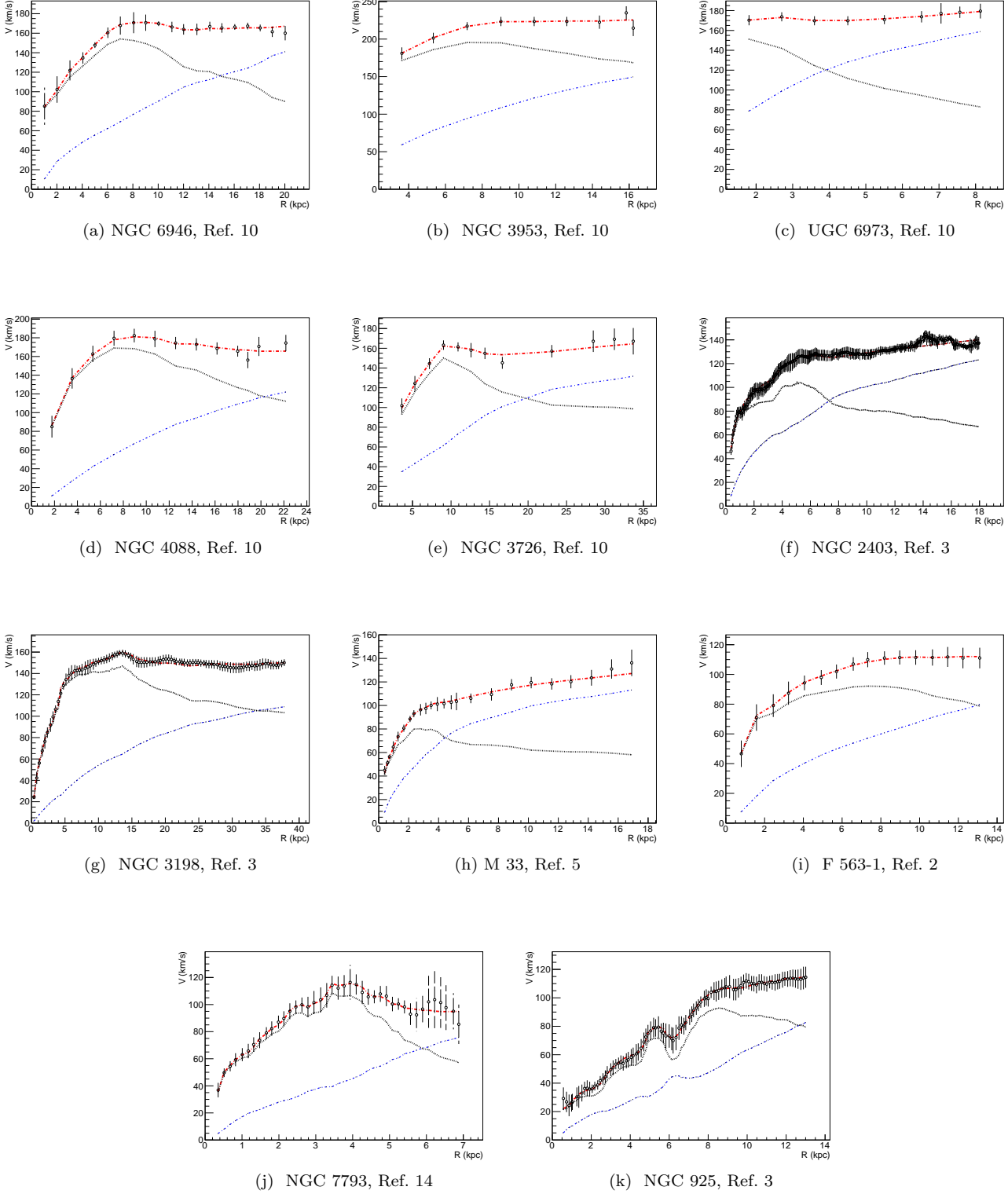


Figure 5. LCM rotation curve fits. In all panels: lines are as in previous figure. References are as in Table 2.

APPENDIX A: LCM HEURISTIC

The most general form of the Lorentz transformation is the exponential mapping:

$$\Lambda = e^x = \sum_{n=0}^{\infty} \frac{x^n}{n!} \quad (\text{A1})$$

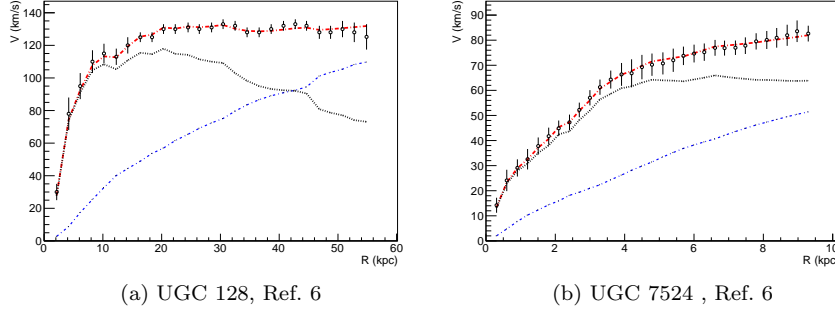


Figure 6. LCM rotation curve fits. In all panels: lines are as in previous figure. References are as in Table 2.

where $\chi = -\xi S$ is the product of the rapidity angle ξ and the generator of the rotation S . The rotation through the angle ξ , for a given action S , defines the relationship between two frames in the hyperbolic space-time of Special Relativity. In the LCM we take the measured photon frequencies to back-out the underlying luminous mass profile using the Lorentz mapping formalism.

The Doppler-shift formula in Eq. 4 comes from such a Lorentz transformation; specifically, rotating a photon's 4-vector (ω, k_i) between two frames, as related by the rapidity angle ξ , for λ the wavelength, $k_i = 2\pi/\lambda_i$, and the indices of the spatial basis $i = 1, 2, 3$. Written geometrically then, the Lorentz Doppler-shift formula is:

$$\frac{v}{c} = \tanh \xi = \frac{e^\xi - e^{-\xi}}{e^\xi + e^{-\xi}}. \quad (\text{A2})$$

We can extend this formalism to a pair of emitter and receiver galaxies by noting that the kernel of this mapping is the ratio of the received to emitted frequency:

$$e^\xi(r) = \omega_{\text{receiver}}(r)/\omega_{\text{emitter}}(r), \quad (\text{A3})$$

and that the diffuse nature of these galactic systems is within the regime of Special Relativity, thus the common use of Newtonian kinematics in the treatment of dark matter analyses.

A0.1 Curved Mapping v_1

The first LCM term, v_1 , looks at the gravitational redshift frequencies $\omega(r)$ (Eq. 8) of the emitter galaxy with respect to those of the receiver galaxy (eg. Milky Way), phrased kinematically as equivalent Doppler-shifts. The kernel for the curved 2-frame map of emitter to the receiver galaxy, is identified with the Schwarzschild gravitational redshifts due to the enclosed luminous mass as a function of radius. It has been shown in Cisneros et al. (2015) that the addition of Kerr-type effects are nominal in these cases, within our current observational capabilities, and so use of the Schwarzschild formalism is sufficient to demonstrate the relative curvature effects.

The curved 2-frame mapping kernel is then:

$$e^{\xi_c}(r) = \frac{\omega_{mw}(r)}{\omega_{gal}(r)}, \quad (\text{A4})$$

for $\omega_{gal}(r)$ and $\omega_{mw}(r)$ respectively the gravitational redshifts of the emitter (*gal*) and receiver galaxies (*mw*) as a function of radius (Eq. 8).

The curved 2-frame convolution function v_1 has been modified from the original form reported in Cisneros et al. (2013) and Cisneros et al. (2014), as we have found a more robust Lorentz-type convolution to involve only the respective clocks of the two galaxies. The term $\gamma^{-1} = \text{sech}(\xi_c) = d\tau/dt$, familiar from Special Relativistic treatments of mass and time dilation, acts to relate the clocks between different frames using shifted photon frequencies as the measure of clock time in the manifold. The more robust 2-frame curvature map v_1 is then:

$$\frac{v_1}{c} = \left(\frac{2}{e^{\xi_c} + e^{-\xi_c}} - 1 \right). \quad (\text{A5})$$

All quantities are functions of radius except for the vacuum light speed.

A0.2 Curved to Flat Mapping v_2

The second LCM term, v_2 , transforms between the curved 2-frame (kernel Eq. A4) to the flat 2-frame. Since all physics measurements are made in our local flat frames, it is necessary to now transform from the previous curved 2-frame map to the flat 2-frame. The reported Keplerian rotation curves $v_{lum}(r)$, which are frequently reported with the observed “flat” rotation curves to show discrepancies at large radius, are our best estimates of these flat-frames and so will be used to define the flat 2-frame.

The shifted frequencies $\omega_l(r)$ expected for $v_{lum}(r)$ are defined by the relation:

$$\frac{v_{lum}(r)}{c} = \frac{\frac{\omega_l(r)}{\omega_o} - \frac{\omega_o}{\omega_l(r)}}{\frac{\omega_l(r)}{\omega_o} + \frac{\omega_o}{\omega_l(r)}}. \quad (\text{A6})$$

Consistent with Eq. A3, the flat 2-frame mapping kernel is:

$$e^{\xi_f}(r) = \frac{\omega_l(r)}{\omega_o}. \quad (\text{A7})$$

Since the v_2 mapping involves four frames (2-frame onto 2-frame) it is algebraically convenient to write it as:

$$(e^{\xi_2})^2 = \frac{e^{\xi_f}}{e^{\xi_c}}, \quad (\text{A8})$$

such that the final term is:

$$\frac{v_2}{c} = \frac{e^{2\xi_2} + 1}{e^{2\xi_2} - 1}, \quad (\text{A9})$$

where all quantities are functions of radius except for the

vacuum speed of light and the characteristic frequency ω_ϕ . We find that this term is most robust when normalized by it's value at large radius, as representative of the value as $r \rightarrow \infty$.

It is important to note that this is essentially an enforced reverse boost, since in Special Relativity Lorentz boosts are always defined as positive rotations away from the rest frame (vertical axis in the light cone compare to Eq. A2), and here we want to transform back *to* the rest frame.

In our quest for every refined measurements of the light distribution from distant objects, the LCM is an empirical construction which predicts rotation curves exceedingly well. In so far as it allows an observationally based and expedient manner in which to discriminate model based predictions, the LCM is a constraint to population synthesis modeling which can expand of our analysis capability.

REFERENCES

- Battaglia G., Fraternali F., Oosterloo T., Sancisi R., 2006, A&A, 447, 49
- Begeman K., 1989, A&A, 223, 47
- Bosma A., 1978, PhD thesis, PhD Thesis, Groningen Univ., (1978)
- Botttema R., Pestana J., Rothberg B., Sanders R., 2002, A&A, 393, 453
- Brun R., Rademakers F., 1997, Nucl. Inst. & Meth. in Phys. Res. A, 389, 81
- Carignan C., Chemin L., 2006, ApJ, 641, L109
- Cisneros S., Goedecke G., Beetle C., Engelhardt M., 2015, Mon.Not.Roy.Astron.Soc., 448, 2733
- Cisneros S., Oblath N., Formaggio J., Goedecke G., Chester D., et al., 2013, ARXIV:1309.7370
- Cisneros S., Oblath N., Formaggio J., Ott R., Chester D., et al., 2014, ARXIV:1407.7583
- Corbelli E., 2003, MNRAS, 342, 199
- de Blok W., Walter F., Brinks E., 2008, AJ, 136, 2648
- Dicaire I., Carignan C., Amram P., Marcelin M., Hlavacek-Larrondo J., et al., 2008, AJ, 135
- Fraternali F., Sancisi R., Kamphuis P., 2011, A&A, <http://arxiv.org/abs/1105.3867>
- Gentile G., Farnaey B., de Blok W., 2011, A&A, 527, A76
- Gentile G., Józsa G. I. G., Serra P., Heald G. H., de Blok W. J. G., Fraternali F., Patterson M. T., Walterbos R. A. M., Oosterloo T., 2013, A&A, 554, A125
- Giraud E., 2000, AJ, 531, 701
- GraphClick 2013, Arizona Software. <http://www.arizona-software.ch/graphclick/>
- Hartle J., 2003, Gravity. Addison-Wesley
- Klypin A., Zhao H., Somerville R., 2002, ApJ, 573, 597
- Mannheim P. D., 2006, Progress in Particle and Nuclear Physics, 56, 340
- Mannheim P. D., O'Brien J. G., 2012, Phys. Rev. D, 85, 124020
- Mannheim P. D., O'Brien J. G., 2013, Journal of Physics Conference Series, 437, 012002
- Milgrom M., 1983, ApJ, 270, 371
- Narayan R., Bartelman M., 1997, Formation of Structure in the Universe: Lectures on Gravitational Lensing. A. Dekel & J. P. Ostriker
- Navarro J., 1998, arxiv:astro-ph/9807084

- Navarro J., Frenk C., White S., 1997, ApJ, 462, 563
- Persic M., Salucci P., Stel F., 1996, MNRAS, 281, 27
- Radosz A., Augousti A. T., Siwek A., 2013, Gen.Rel.Grav., 45, 705
- Randriamampandry T. H., Carignan C., 2014, MNRAS, 439, 2132
- Rubin V. C., Thonnard N., Ford Jr. W. K., 1978, ApJ, 225, L107
- Sanders R., 1996, ApJ, 473, 117
- Sanders R., McGaugh S., 2002, ARA&A, 40, 263
- Sofue Y., 2013, Mass Distribution and Rotation Curve in the Galaxy. Oswald, T. D. and Gilmore, G., p. 985
- Xue X., et al., 2008, AJ., 684, 1143

This paper has been typeset from a \TeX / \LaTeX file prepared by the author.